J|A|C|S
ARTICLES
Published on Web 04/12/2003

Electrospray Ionization Fourier Transform Ion Cyclotron Resonance Mass Spectrometric Analysis of Metal-Ion Selected Dynamic Protein Libraries

Helen J. Cooper,[†] Martin A. Case,[‡] George L. McLendon,*[,‡] and Alan G. Marshall*[,†]

Contribution from the Ion Cyclotron Resonance Program, National High Magnetic Field Laboratory, Florida State University, 1800 East Paul Dirac Drive, Tallahassee, Florida 32310-3706, and Department of Chemistry, Princeton University, Princeton, New Jersey 08544

Received August 30, 2002; E-mail: glm@princeton.edu; marshall@magnet.fsu.edu

Abstract: The application of electrospray ionization (ESI) Fourier transform ion cyclotron resonance (FT-ICR) mass spectrometry to the investigation of the relative stabilities (and thus packing efficiencies) of Fe-bound trihelix peptide bundles is demonstrated. Small dynamic protein libraries are created by metal-ion assisted assembly of peptide subunits. Control of the trimeric aggregation state is coupled to stability selection by exploiting the coordination requirements of Fe^{2+} in the presence of bidentate 2,2′-bipyridyl ligands covalently appended to the peptide monomers. At limiting metal-ion concentration, the most thermodynamically stable, optimally packed peptide trimers dominate the mass spectrum. The identities of optimally stable candidate trimers observed in the ESI FT-ICR mass spectra are confirmed by resynthesis of exchange-inert analogues and measurement of their folding free energies. The peptide composition of the trimers may be determined by infrared multiphoton dissociation (IRMPD) MS^3 experiments. Additional sequence information for the peptide subunits is obtained from electron capture dissociation (ECD) of peptides and metal-bound trimers. The experiments also suggest the presence of secondary structure in the gas phase, possibly due to partial retention of the solution-phase coiled coil structure.

Introduction

Traditional combinatorial libraries comprise large numbers of species, which are first synthesized and then screened for the feature of interest. Dynamic, or virtual, combinatorial libraries represent a fundamentally different approach. Such libraries are created through the self-assembly (either noncovalent or covalent) of smaller components. For a given set of components, all possible structural combinations in both nature (e.g., type of interaction) and number (e.g., degree of oligomerization) are *virtually* available. The species that *actually* dominate the distribution are those that are the thermodynamically most stable. In other words, a dynamic combinatorial library will self-screen for stability. The concept of dynamic combinatorial libraries and their potential role in drug discovery has been reviewed extensively.[1−9] Most applications exploit a template (usually the protein binding domain of interest) to which an equilibrium population of protoligand subunits can bind noncovalently. The population of molecules bound to the template will be dominated by those subunits that thermodynamically best complement the template. Identification of these library members entails covalent capture of the ligand assembly[10,11] or sufficiently kinetically inert products[12−15] to allow interrogation of the selected ligands by techniques such as

[†] Department of Chemistry and Biochemistry, Florida State University, and National High Magnetic Field Laboratory.

[‡] Princeton University.

(1) Rowan, S. J.; Cantrill, S. J.; Cousins, G. R. L.; Sanders, J. K. M.; Stoddart, J. F.; Dynamic covalent chemistry. *Angew. Chem., Int. Ed.* **2002**, *41*, 898−952.
(2) Lehn, J.-M. Dynamic combinatorial chemistry and virtual combinatorial libraries. *Chem.—Eur. J.* **1999**, *5*, 2455−2463.
(3) Otto, S.; Furlan, R. L. E.; Sanders, J. K. M. Dynamic combinatorial chemistry. *Drug Discovery Today* **2002**, *7*, 117−125.
(4) Otto, S.; Furlan, R. L. E.; Sanders, J. K. M. Recent developments in dynamic combinatorial chemistry. *Curr. Opin. Chem. Biol.* **2002**, *6*, 321−327.
(5) Huc, I.; Nguyen, R. Dynamic combinatorial chemistry. *Comb. Chem. High Throughput Screening* **2001**, *4*, 53−74.
(6) Eliseev, A. V.; Lehn, J.-M. Dynamic combinatorial chemistry: Evolutionary formation and screening of molecular libraries. *Curr. Top. Microbiol.* **1999**, *243*, 159−172.
(7) Ganesan, A. Strategies for the dynamic integration of combinatorial synthesis and screening. *Angew. Chem., Int. Ed.* **1998**, *37*, 2828−2831.
(8) Brady, P. A.; Sanders, J. K. M. Selection approaches to catalytic systems. *Chem. Soc. Rev.* **1997**, *26*, 327−336.
(9) Klekota, B.; Miller, B. J. Dynamic diversity and small molecule evolution: a new paradigm for ligand identification. *Trends Biotechnol.* **1999**, *17*, 205−209.
(10) Clark, T. D.; Ghadiri, M. R. Supramolecular design by covalent capture: Design of a peptide cylinder via hydrogen bond promoted intermolecular olefin metathesis. *J. Am. Chem. Soc.* **1995**, *117*, 12364−12365.
(11) Huc, I.; Lehn, J.-M. Virtual combinatorial libraries: Dynamic generation of molecular and supramolecular diversity by self assembly. *Proc. Natl. Acad. Sci. U.S.A.*, **1997**, *94*, 2106−2110.
(12) Otto, S.; Furlan, R. L. E.; Sanders, J. K. M. Dynamic combinatorial libraries of macrocyclic disulfides in water. *J. Am. Chem. Soc.* **2000**, *122*, 12063−12064.
(13) Nazarpack-Kandlousy, N.; Zwiegenbaum, J.; Henion, J.; Eliseev, A. V. Synthesis and characterization of a mixture-based library of oxime ethers based on a common aromatic scaffold. *J. Comb. Chem.* **1999**, *1*, 199−206.
(14) Ramstrom, O.; Lehn, J.-M. In situ generation and screening of a dynamic combinatorial carbohydrate library against concanavalin A. *ChemBioChem* **2000**, *1*, 41−48.
(15) Cousins, G. R. L.; Furlan, R. L. E.; Ng, Y.-F.; Redman, J. E.; Sanders, J. K. M. Identification and isolation of a receptor for N-methyl alkylammonium salts: Molecular amplification in a pseudo-peptide dynamic combinatorial library. *Angew. Chem., Int. Ed.* **2001**, *40*, 423−428.

10.1021/ja021138f CCC: $25.00

nuclear magnetic resonance (NMR) and mass spectrometry (MS). The latter approach is particularly suited to the task, because high-resolution mass spectrometry may be performed on picomoles of sample, in the presence of the template and any reagents used to effect the covalent capture.[12,16−19]

A dynamic combinatorial strategy for exploring the factors underlying the efficient packing of protein interiors was the subject of a previous communication.[20] The folding stability of a small, globular protein is largely governed by the packing of the hydrophobic core in ways that are not fully understood. It remains unclear whether optimal stability is conferred by desolvation of the maximum hydrophobic surface upon folding or that more intimate packing of the hydrophobic side chains plays a dominant role.[21,22] Small peptide subunits (20−25 amino acids) are designed to fold into amphiphilic α-helices according to well-established principles.[23−28] A conserved, minimal array of hydrophilic amino acids is employed to describe the exterior of an assembled trimeric structure, and the interior hydrophobic amino acids are allowed to differ among library members. Each peptide has a bidentate 2,2′,5-carboxybipyridyl ligand appended covalently by means of an amide linkage to the N-terminus. Addition of ferrous iron sequesters three such ligands to form the octahedral $[Fe(bpy)_3]^{2+}$ complex. Formation of the complex increases the effective local peptide concentration, and the ensuing hydrophobic collapse of the interior of the structure is accompanied by folding of the tertiary parallel trihelix bundle protein.

At limiting ferrous iron concentration, only those peptides that together constitute optimally stable trihelix bundles are sequestered. We have previously described[20] how such a library may be screened by size-exclusion chromatography to separate the small population of trimers from the bulk of uncomplexed monomers. Mass spectrometric analysis of the heavy fraction permitted identification of the constituent monomers, and resynthesis of candidate trimers as their exchange-inert ruthenium(II) analogues permitted folding free energies to be determined explicitly and thus confirmed that the process did indeed select for optimal stability. However, it should be noted that at no time during the experiment were any of the iron(II) trihelix bundles observed directly. As may be imagined, deconvolution of a larger library by this approach presents a formidable challenge, the meeting of which necessitates recursive sublibrary investigation and stability studies requiring the resynthesis of exchange-inert candidate trimers.

In a first step toward circumventing these difficulties, we here investigate small dynamic libraries of $[Fe(peptide)_3]^{2+}$ trihelix bundles by use of electrospray ionization (ESI)[29−32] Fourier transform ion cyclotron resonance (FT-ICR)[33,34] mass spectrometry. ESI is a gentle ionization technique that allows the generation of intact noncovalent complexes in the gas phase,[35,36] a feature that has been exploited for the screening of traditional combinatorial libraries, e.g., competitive binding of members of a ligand library to a protein.[37−40] FT-ICR mass spectrometry provides high mass resolution and mass accuracy, making it ideal for analyzing complex mixtures such as combinatorial libraries, and the technique has previously been applied to the analysis of dynamic libraries.[12,16] The results presented here show direct mass spectrometric observation of the trihelix bundles. By limiting the concentration of iron(II), we are able to ascertain the relative stabilities of the trihelix bundles and hence gain insight into their packing efficiencies. Two studies are presented. The first explores a library in which all members are folded in solution at pH 6 and in which the differential free energies of folding are modest (a few hundred calories). A minimal dynamic library of four species assembled from two peptides αpL (Bpy-GELAQKLEQALQKLEQALQK-NH_2) and αpL_{V1} (Bpy-GQAVQKLEQALQKLEQALQK-NH_2) was investigated. Circular dichroism experiments suggest that the homotrimers of αpL and αpL_{V1} both adopt a coiled-coil fold. α-Helical coiled coils[41] consist of a regularly repeating heptad

(16) Poulsen, S. A.; Gates, P. G.; Cousins, G. R. L.; Sanders, J. K. M. Electrospray ionisation FTICR MS of dynamic combinatorial libraries. *Rapid Commun. Mass Spectrom.* **2000**, *14*, 44−48.
(17) Schmid, D. G.; Grosche, P.; Bandel, H.; Jung, G. FTICR mass spectrometry for high resolution analysis in combinatorial chemistry. *Biotechnol. Bioeng.* **2001**, *71*, 151−161.
(18) Schmid, D. G.; Grosche, P.; Jung, G. High resolution analysis of a 144-membered pyrazole library from combinatorial solid phase synthesis by using electrospray ionization FTICR. *Rapid Commun. Mass Spectrom.* **2001**, *15*, 341−347.
(19) Shin, Y. G.; van Breeman, R. B. Analysis and screening of combinatorial libraries using mass spectrometry. *Biopharm. Drug Dispos.* **2001**, *22*, 353−372.
(20) Case, M. A.; McLendon, G. L. A virtual library approach to investigate protein folding and internal packing. *J. Am. Chem. Soc.* **2000**, *122*, 8089−8090.
(21) Beasley, J. R.; Hecht, M. H. Protein design: The choice of de novo sequences. *J. Biol. Chem.* **1997**, *272*, 2031−2034.
(22) Lazar, G. A.; Handel, T. M. Hydrophobic core packing and protein design. *Curr. Opin. Chem. Biol.* **1998**, *2*, 675−679.
(23) Micklatcher, C.; Chmielewski, J. Helical peptide and protein design. *Curr. Opin. Chem. Biol.* **1999**, *3*, 724−729.
(24) Kohn, W. D.; Hodges, R. S. De novo design of α-helical coiled coils and bundles: models for the development of protein design principles. *Trends Biotechnol.* **1998**, *16*, 379−389.
(25) Woolfson, D. N. Core-directed protein design. *Curr. Opin. Struct. Biol.* **2001**, *11*, 464−471.
(26) Harbury, P. B.; Zhang, T.; Kim, P. S.; Alber, T. A switch between 2-stranded, 3-stranded and 4-stranded coiled-coils in GCN4 leucine zipper mutants. *Science* **1993**, *262*, 1401−1407.
(27) Ghadiri, M. R.; Soares, C.; Choi, C. A convergent approach to protein design. Metal-ion assisted spontaneous self-assembly of a polypeptide into a triple helix bundle protein. *J. Am. Chem. Soc.* **1992**, *114*, 825−831.
(28) Case, M. A.; Ghadiri, M. R.; Mutz, M. W.; McLendon, G. L. Stereoselection in designed three-helix bundle metalloproteins. *Chirality* **1998**, *10*, 35−40.
(29) Fenn, J. B.; Mann, M.; Meng, C. K.; Wong, S. F.; Whitehouse, C. M. Electrospray ionization for mass spectrometry of large biomolecules. *Science* **1989**, *246*, 64−71.
(30) Smith, R. D.; Loo, J. A.; Ogorzalek Loo, R. R.; Busman, M.; Udseth, H. R. Electrospray MS Review. *Mass Spectrom. Rev.* **1991**, *10*, 359−451.
(31) Hendrickson, C. L.; Emmett, M. R. Electrospray ionization Fourier transform ion cyclotron resonance mass spectrometry. *Annu. Rev. Phys. Chem.* **1999**, *50*, 517−536.
(32) Lorenz, S. A.; Maziarz, E. P. I.; Wood, T. D. Electrospray ionization Fourier transform mass spectrometry of macromolecules: The first decade. *Appl. Spectrosc.* **1999**, *53*, 18A−36A.
(33) Marshall, A. G.; Hendrickson, C. L.; Jackson, G. S. Fourier transform ion cyclotron resonance mass spectrometry: A primer. *Mass Spectrom. Rev.* **1998**, *17*, 1−35.
(34) Comisarow, M. B.; Marshall, A. G. Fourier transform ion cyclotron resonance spectroscopy. *Chem. Phys. Lett.* **1974**, *25*, 282−283.
(35) Loo, J. A. Studying non-covalent protein complexes by electrospray ionization mass spectrometry. *Mass Spectrom. Rev.* **1997**, *16*, 1−23.
(36) Smith, R. D.; Light-Wahl, K. J. The observation of non-covalent interactions in solution by electrospray ionization mass spectrometry—promise, pitfalls and prognosis. *Biol. Mass Spectrom.* **1993**, *22*, 493−501.
(37) Cheng, X.; Chen, R.; Bruce, J. E.; Schwartz, B. L.; Anderson, G. A.; Hofstadler, S. A.; Gale, D. C.; Smith, R. D.; Gao, J.; Sigal, G. B.; Mammen, M.; Whitesides, G. M. Using electrospray FT-ICR mass spectrometry to study competitive binding of inhibitors to carbonic anhydrase. *J. Am. Chem. Soc.* **1995**, *117*, 8859−8860.
(38) Gao, J.; Cheng, X.; Chen, R.; Sigal, G. B.; Bruce, J. E.; Schwartz, B. L.; Hofstadler, S. A.; Anderson, G. A.; Smith, R. D.; Whitesides, G. M. Screening derivatized peptide libraries for tight binding inhibitors to carbonic anhydrase II by electrospray ionization mass spectrometry. *J. Med. Chem.* **1996**, *39*, 1949−1955.
(39) Loo, J. A.; Hu, P.; McConnell, P.; Mueller, W. T.; Sawyer, T. K.; Thanabal, V. A study of Src SH2 domain protein−phosphopeptide binding interactions by electrospray ionization mass spectrometry. *J. Am. Soc. Mass Spectrom.* **1997**, *8*, 234−243.
(40) Wigger, M.; Eyler, J. R.; Benner, S. A.; Li, W.; Marshall, A. G. Fourier transform ion cyclotron resonance mass spectrometric identification and screening of non-covalent complexes Hck Src homology 2 domain receptor and ligands from a 324 peptide combinatorial library. *J. Am. Soc. Mass Spectrom.* **2002**, *13*, 1162−1169.

unit designated abcdefg, in which positions a and d are occupied predominantly by hydrophobic amino acids and positions e and g are predominantly charged residues. The heptad repeats in the peptides described commence at position 4; i.e., the first a-postion residue in peptide αpL is alanine, and it is valine in peptide αpL_{V1}. Both peptides are leucine-rich at the a- and d-positions; however, circular dichroism experiments suggest that the latter arrangement $(\alpha pL_{V1})_3$ is less stable than the $(\alpha pL)_3$ analogue. The ESI FT-ICR MS results for this library reflect the solution-phase equilibrium exchange data.

In our second study, the 11-member dynamic library (assembled from peptides αpL, αpLA, and αpA) described by Case and McLendon[20] is revisited. Circular dichroism studies of the exchange-inert ruthenium analogues of the candidate trimers suggest that only $[Ru(\alpha pL)_3]^{2+}$ and $[Ru(\alpha pL)_2(\alpha pLA)]^{2+}$ adopt the coiled-coil fold. The remaining trimers showed little or no α-helicity. Unfolding studies of $[Ru(\alpha pL)_3]^{2+}$ and $[Ru(\alpha pL)_2(\alpha pLA)]^{2+}$ revealed folding free energies, ΔG_{fold}, of −3.0 and −2.4 kcal mol^{-1}, respectively. Thus, in contrast with the first study, this library comprises members with a wide range of folding free energies (several kcal), thereby raising an interesting question. At high Fe(II) concentration, chelation of the peptides that *do not* assume trihelical folds is possible. Will unstable nonhelical trimers be observed in the mass spectra? The present results suggest that although ESI FT-ICR MS measurements do not in this case necessarily reflect solution-phase equilibrium distributions, they do allow identification of stable trihelix bundles and reveal the variations in stabilities of these structures. This observation reveals an unexpected advantage in the application of this technique to screening of dynamic libraries as a method of addressing the question of optimal packing in trihelix bundles in that unfolded structures are effectively filtered out of the analysis.

We also performed infrared multiphoton dissociation (IRMPD)[42,43] and electron capture dissociation (ECD)[44,45] of several trimeric species. These experiments were undertaken with a view to enabling characterization of larger dynamic libraries: i.e., once an optimally stable bundle has been identified, one would fragment the complex to learn about the peptide subunit amino acid sequence. In addition to providing sequence information, the dissociation data suggest that the trimeric species exhibit some secondary structure in the gas phase. An obvious explanation for this observation is (partial) retention of solution-phase structure.

Experimental Methods

Samples. Peptides αpL (Bpy-GELAQKLEQALQKLEQALQK-NH_2), αpLA (Bpy-GELAQKAEQALQKAEQALQK-NH_2), αpA (Bpy-GELAQKAEQAAQKAEQAAQK-NH_2), αpL_{V1} (Bpy-GQAVQKLEQALQKLEQALQK-NH_2), and αpVL (Bpy-GQAVQKLEQAVQKLEQAVQKLEQA-NH_2) were synthesized with N-terminal 2,2′-bipyridyl moieties, as described elsewhere.[20] The samples were electrosprayed from solutions of ammonium acetate (Aldrich, Milwaukee, WI) in water (5 mM) or 1:1 water/methanol (J. T. Baker, Philipsburg, NJ), 2% acetic acid (Aldrich, Milwaukee, WI). For each library, individual peptide concentrations were 10 μM. Fe(II) was added as ferrous ammonium sulfate (Aldrich, Milwaukee, WI) at varying concentrations (see below). Unfolding studies were performed on ruthenium(II) trihelix bundles, the synthesis of which has also been described elsewhere.[20]

FT-ICR Mass Spectrometry. Peptide samples were analyzed with a home-built, passively shielded, 9.4 T FT-ICR mass spectrometer[46] equipped with an external microelectrospray ionization source.[47] The samples were infused at a flow rate of 1 μL/min through an electrospray emitter consisting of a 50 μm i.d. fused silica capillary that had been mechanically ground to a uniform thin-walled tip.[48] A 2.2 kV potential was applied between the microspray emitter and the capillary entrance. The electrosprayed ions were delivered into the mass spectrometer through a Chait-style atmosphere-to-vacuum interface[49] and were externally accumulated[47] for 5 s in an rf-only octapole. The ions were transferred through multipole ion guides and trapped in an open[50] cylindrical cell (Malmberg-Penning trap[51]).

Ions were frequency-sweep ("chirp")[52] excited (41−320 kHz at 150 Hz/μs) and detected in direct mode (512 kword time-domain data). Between 10 and 20 time-domain data sets were co-added, Hanning apodized, zero-filled once, and subjected to fast Fourier transform (FFT) followed by magnitude calculation. The experimental event sequence was controlled by a modular ICR data acquisition system (MIDAS).[53] The FT-ICR mass spectra were internally frequency-to-*m*/*z*-calibrated[54,55] with respect to doubly and triply charged peptide monomers. The FT-ICR mass spectra were analyzed by use of the MIDAS analysis software package.[56]

Infrared Multiphoton Dissociation and Electron Capture Dissociation. Stored-waveform inverse Fourier transform (SWIFT)[57−59]

(41) Crick, F. H. C. The packing of α-helices: Simple coiled-coils. *Acta Crystallogr.* **1953**, *6*, 689−698.
(42) Woodlin, R. L.; Bomse, D. S.; Beauchamp, J. L. Multiphoton dissociation of molecules with low power continuous wave infrared laser radiation. *J. Am. Chem. Soc.* **1978**, *100*, 3248−3250.
(43) Little, D. P.; Speir, J. P.; Senko, M. W.; O'Connor, P. B.; McLafferty, F. W. Infrared multiphoton dissociation of large multiply charged ions for biomolecule sequencing. *Anal. Chem.* **1994**, *66*, 2809−2815.
(44) Zubarev, R. A.; Kelleher, N. L.; McLafferty, F. W. Electron capture dissociation of multiply charged protein cations. A nonergodic process. *J. Am. Chem. Soc.* **1998**, *120*, 3265−3266.
(45) McLafferty, F. W.; Horn, D. M.; Breuker, K.; Ge, Y.; Lewis, M. A.; Cerda, B.; Zubarev, R. A.; Carpenter, B. K. Electron capture dissociation of gaseous multiply charged ions by Fourier transform ion cyclotron resonance. *J. Am. Soc. Mass Spectrom.* **2001**, *12*, 245−249.
(46) Senko, M. W.; Hendrickson, C. L.; Pasa-Tolic, L.; Marto, J. A.; White, F. M.; Guan, S.; Marshall, A. G. Electrospray ionization FT-ICR mass spectrometry at 9.4 Tesla. *Rapid Commun. Mass Spectrom.* **1996**, *10*, 1824−1828.
(47) Senko, M. W.; Hendrickson, C. L.; Emmett, M. R.; Shi, S. D.-H.; Marshall, A. G. External accumulation of ions for enhanced electrospray ionization Fourier transform ion cyclotron resonance mass spectrometry. *J. Am. Soc. Mass Spectrom.* **1997**, *8*, 970−976.
(48) Quinn, J. P.; Emmett, M. R.; Marshall, A. G. *Proceedings of the 46th ASMS Conference on Mass Spectrometry and Allied Topics*, Orlando, FL, May 31−June 4, 1998; American Society for Mass Spectrometry: Sante Fe, NM, 1998; pp 1388−1388.
(49) Chowdhury, S. K.; Katta, V.; Chait, B. T. An electrospray-ionization mass spectrometer with new features. *Rapid Commun. Mass Spectrom.* **1990**, *4*, 81−87.
(50) Beu, S. C.; Laude, D. A., Jr. Open trapped ion cell geometries for FT-ICR MS. *Int. J. Mass Spectrom. Ion Processes* **1992**, *112*, 215−230.
(51) Malmberg, J. H.; O'Neil, T. M. Pure electron plasma, liquid, and crystal. *Phys. Rev. Lett.* **1977**, *39*, 1333−1336.
(52) Marshall, A. G.; Roe, D. C. Theory of Fourier transform ion cyclotron resonance mass spectrospcopy: Response to frequency sweep excitation. *J. Chem. Phys.* **1980**, *73*, 1581−1590.
(53) Senko, M. W.; Canterbury, J. D.; Guan, S.; Marshall, A. G. A high-performance modular data system for FT-ICR mass spectrometry. *Rapid Commun. Mass Spectrom.* **1996**, *10*, 1839−1844.
(54) Ledford, E. B., Jr.; Rempel, D. L.; Gross, M. L. Space charge effects in Fourier transform mass spectrometry. Mass calibration. *Anal. Chem.* **1984**, *56*, 2744−2748.
(55) Shi, S. D.-H.; Drader, J. J.; Freitas, M. A.; Hendrickson, C. L.; Marshall, A. G. Comparison and interconversion of the two most common frequency-to-mass calibration functions for Fourier transform ion cyclotron resonance mass spectrometry. *Int. J. Mass Spectrom.* **2000**, *195/196*, 591−598.
(56) Blakney, G. T.; van der Rest, G.; Johnson, J. R.; Freitas, M. A.; Drader, J. J.; Shi, S. D.-H.; Hendrickson, C. L.; Kelleher, N. L.; Marshall, A. G. *Proceedings of the 49th ASMS and Allied Topics*, Chicago, IL, May 28−31, 2001; American Society for Mass Spectrometry: Sante Fe, NM, 2001; WPM265.
(57) Marshall, A. G.; Wang, T.-C. L.; Ricca, T. L. Tailored excitation for Fourier transform ion cyclotron resonance mass spectrometry. *J. Am. Chem. Soc.* **1985**, *107*, 7893−7897.
(58) Wang, T.-C. L.; Ricca, T. L.; Marshall, A. G. Extension of dynamic range in Fourier transform ion cyclotron resonance mass spectrometry via stored waveform inverse Fourier transform excitation. *Anal. Chem.* **1986**, *58*, 2935−2938.

ejection served to isolate the species under investigation. A dispenser cathode electron gun (HeatWave, Watsonville, CA)[60,61] installed ~1 m behind the FT-ICR cell provided the electrons for electron capture dissociation (ECD).[44,45] Throughout most of the experimental event sequence, a potential of +10 V was applied to the cathode. During the ECD event, that potential was −0.13 V. A grid situated in front of the filament was kept at −10 V for most of the experiment and pulsed to +20 V during the ECD event. The isolated parent ions were irradiated with electrons for 2 s. Each ECD spectrum was derived from the sum of 120 or 200 time-domain transients. A continuous wave 40 W, 10.6 μm wavelength CO_2 laser (Synrad E48-2-115, Bothell, WA) fitted with a beam expander provided the photons for infrared multiphoton dissociation (IRMPD).[42,43] The laser beam is directed to the center of the ICR cell through a BaF_2 window. Photon irradiation was performed for 1 s at 10−50% laser power. The IRMPD spectra presented represent an average of 5−20 time-domain transients. IRMPD FT-ICR mass spectra were internally frequency-to-*m*/*z*-calibrated[54,55] with respect to the doubly charged peptide monomer and the parent trimer ions. IRMPD MS^3 FT-ICR mass spectra were externally calibrated with respect to an electrospray tuning mix (Agilent Technologies, Wilmington, DE).

Modeling of Trimer Distributions. The free energy of trihelix formation is made up of two terms, the intrinsic free energy of formation of the $Fe(bpy)_3$ complex (adjusted for the loss of free energy due to the entropic cost of exclusive formation of facial isomers[62,63]) and the trihelix folding free energy.

$$\Delta G_{\text{total}} = \Delta G_{\text{complex}} + \Delta G_{\text{fold}} \quad (1)$$

The complexes assemble according to

$$3\alpha\text{pL} + \text{Fe}^{2+} \underset{K_1}{\rightleftharpoons} 2\alpha\text{pL} + [\text{Fe}(\alpha\text{pL})]^{2+} \underset{K_2}{\rightleftharpoons} \alpha\text{pL} + [\text{Fe}(\alpha\text{pL})_2]^{2+} \underset{K_3}{\rightleftharpoons} [\text{Fe}(\alpha\text{pL})_3]^{2+} \quad (2)$$

For iron(II) trisbipyridyl complexes, $K_1 < K_2 \ll K_3$ and the system can be treated as a one-step process:

$$3\alpha\text{pL} + \text{Fe}^{2+} \underset{\beta_3}{\rightleftharpoons} [\text{Fe}(\alpha\text{pL})_3]^{2+} \quad (3)$$

in which $\beta_3 = K_1K_2K_3$.

For the trihelix bundle $[Ni(\alpha pL)_3]^{2+}$, β_3 has been measured[63] as 43.5×10^{15} M^{-3}. The stability of the iron(II) complex may be presumed to be similar.[64] From $\Delta G = -RT \log_e K$, the free energy of formation is $\Delta G_{\text{total}} = -22.6$ kcal mol^{-1}. For the exchange-inert analogue $[Ru(\alpha pL)_3]^{2+}$, $\Delta G_{\text{fold}} = -3.0$ kcal mol^{-1}, so the free energy contribution from complex formation is $\Delta G_{\text{complex}} \approx -20$ kcal mol^{-1}. In the following coupled equilibria, the constants β_{i3}, β_{j3}, etc. are the sums of $\Delta G_{\text{complex}} = -20$ kcal mol^{-1} and the folding free energies of the respective trihelix bundles. For the equilibria in which two peptides P_i and P_j form trihelix bundles upon complexation with a metal M, the mass balance equations may be solved iteratively.

The mass balance equations at iteration $n = 1$ are

$$\sum[P_i]_n = [P_i] + 3\beta_{i3}[P_i]^3[M] + 2\beta_{i2j}[P_i]^2[P_j][M] + \beta_{ij2}[P_i][P_j]^2[M]$$

$$\sum[P_j]_n = [P_j] + 3\beta_{j3}[P_j]^3[M] + \beta_{i2j}[P_i]^2[P_j][M] + 2\beta_{ij2}[P_i][P_j]^2[M]$$

$$\sum[M]_n = [M] + \beta_{i3}[P_i]^3[M] + \beta_{j3}[P_j]^3[M] + \beta_{i2j}[P_i]^2[P_j][M] + \beta_{ij2}[P_i][P_j]^2[M]$$

in which β_{i3} is the equilibrium constant for

$$M^{2+} + 3P_i \rightleftharpoons [M(P_i)_3]^{2+}$$

β_{i2j} is the equilibrium constant for

$$M^{2+} + 2P_i + P_j \rightleftharpoons [M(P_i)_2(P_j)]^{2+}$$

β_{ij2} is the equilibrium constant for

$$M^{2+} + 2P_j + P_i \rightleftharpoons [M(P_j)_2(P_i)]^{2+}$$

and β_{j3} is the equilibrium constant for

$$M^{2+} + 3P_j \rightleftharpoons [M(P_j)_3]^{2+}$$

$[P_i]$, $[P_j]$, and [M] are the concentrations of peptides P_i and P_j and the metal ion M^{2+}. Starting values for $[P_i]$, $[P_j]$, and [M] are arbitrary estimates.

The errors in mass balance are

$$\delta[P_i]_n = [P_i]_{\text{total}} - \sum[P_i]_n$$

$$\delta[P_j]_n = [P_j]_{\text{total}} - \sum[P_j]_n$$

$$\delta[M]_n = [M]_{\text{total}} - \sum[M]_n$$

in which $[P_i]_{\text{total}}$, $[P_j]_{\text{total}}$, and $[M]_{\text{total}}$ are known concentrations of peptides P_i and P_j and metal ion M^{2+}.

The first differential of error functions are the following:

$$\delta[P_i]_n' = 1 + 9\beta_{i3}[P_i]^2[M] + 4\beta_{i2j}[P_i][P_j][M] + \beta_{ij2}[P_j]^2[M]$$

$$\delta[P_j]_n' = 1 + 9\beta_{j3}[P_j]^2[M] + \beta_{i2j}[P_i]^2[M] + 4\beta_{ij2}[P_i][P_j][M]$$

$$\delta[M]_n' = 1 + \beta_{i3}[P_i]^3 + \beta_{j3}[P_j]^3 + \beta_{i2j}[P_i]^2[P_j] + \beta_{ij2}[P_i][P_j]^2$$

The Newton−Raphson minimizations are the following:

$$[P_i]_{n+1} = [P_i]_n - \delta[P_i]_n/\delta[P_i]_n'$$

$$[P_j]_{n+1} = [P_j]_n - \delta[P_j]_n/\delta[P_j]_n'$$

$$[M]_{n+1} = [M]_n - \delta[M]_n/\delta[M]_n'$$

The mass-balance equations were rebuilt by use of $(n + 1)$th values, and the process was repeated until convergence. The distribution of trimers is thus returned from knowledge of β, $[P]_{\text{total}}$, and $[M]_{\text{total}}$.

Results and Discussion

Formation of Fe-Bound Trimers. Observation of the trimeric species requires electrospray from water or ammonium acetate solution. Figure 1 (top) shows the mass spectrum

(59) Guan, S.; Marshall, A. G. Stored waveform inverse Fourier transform (SWIFT) ion excitation in trapped-ion mass spectrometry: Theory and applications. *Int. J. Mass Spectrom. Ion Processes* **1996**, *157/158*, 5−37.
(60) Quinn, J. P.; Hakansson, K.; McFarland, M. A.; Hendrickson, C. L.; Marshall, A. G. Presented at the 50th ASMS Conference on Mass Spectrometry and Allied Topics, Orlando, FL, June 2−6, 2002.
(61) Tsybin, Y. O.; Hakansson, P.; Budnik, B. A.; Haselmann, K. F.; Kjeldsen, F.; Gorshkov, M.; Zubarev, R. A. Improved low energy electron injection systems for high rate electron capture dissociation in FTICR MS. *Rapid Commun. Mass Spectrom.* **2001**, *15*, 1849−1854.
(62) Jencks, W. P. On the attribution and additivity of binding energies. *Proc. Natl. Acad. Sci. U.S.A.* **1981**, *78*, 4046−4050.
(63) Gochin, M.; Khorosheva, V.; Case, M. A. Structural characterization of a paramagnetic metal-ion-assembled three-stranded α-helical coiled coil. *J. Am. Chem. Soc.* **2002**, *124*, 11018−11028.
(64) Irving, H.; Mellor, D. H. Stability of metal complexes of 1,10 phenanthroline and its analogues. 1,10 phenanthroline and 2, 2' bipyridyl. *J. Chem. Soc.* **1962**, 5222−5237.

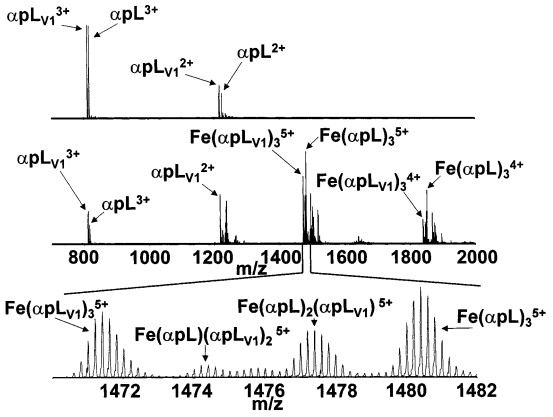

Figure 1. Electrospray ionization Fourier transform ion cyclotron resonance (ESI FT-ICR) mass spectra obtained from samples containing peptide αpL (10 μM), peptide αpL_{V1} (10 μm), and ferrous iron (4 μM) in 1:1 methanol/water, 2% acetic acid (top) and ammonium acetate solution (5 mM) (middle). The bottom panel shows an *m*/*z* scale expansion of the 5+ charge state of Fe-bound trimers from the middle spectrum.

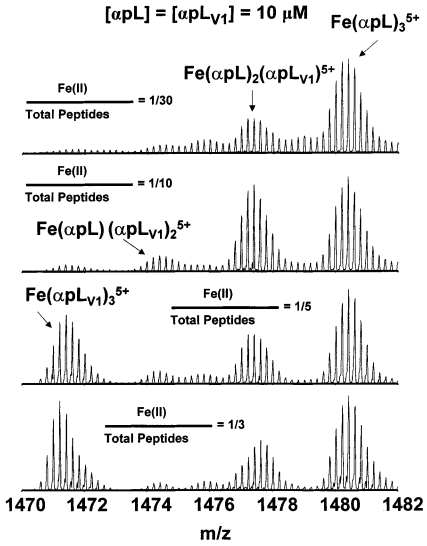

Figure 2. Mass spectral segments showing 5+ charge state of Fe-bound trimers obtained from samples containing peptides αpL (10 μM) and αpL_{V1} (10 μM) and (proceeding from top to bottom) 0.67 μM Fe(II), 2 μM Fe(II), 4 μM Fe(II), and 6.7 μM Fe(II).

obtained from the peptide mixture, αpL (monoisotopic mass, 2446.3330 Da) (10 μM) and αpL_{V1} (monoisotopic mass, 2431.3335 Da) (10 μM) with $^1/_5$ total peptide equivalent (TPE), i.e., 4 μM, of Fe^{2+}, electrosprayed from 1:1 water/methanol and 2% acetic acid. Peaks corresponding to monomeric doubly and triply charged species are observed at *m*/*z* 816.45 and 1224.17 (αpL) and *m*/*z* 811.45 and 1216.67 (αpL_{V1}). No Fe-bound trimers are observed. Presumably, the low pH of the standard electrospray solution (water/methanol and ~2% acetic acid) disrupts the complex. Figure 1 (middle) shows the mass spectrum obtained from the same mixture electrosprayed from ammonium acetate solution. The main peaks in this spectrum correspond to the Fe-bound trimers in the 5+ charge state (see Figure 1 (bottom)). The measured mass-to-charge ratios (1470.58 for $[^{56}Fe(\alpha pL_{V1})_3 + 3H]^{5+}$, 1473.59 for $[^{56}Fe(\alpha pL_{V1})_2(\alpha pL) + 3H]^{5+}$, 1476.59 for $[^{56}Fe(\alpha pL)_2(\alpha pL_{V1}) + 3H]^{5+}$, and 1479.59 for $[^{56}Fe(\alpha pL)_3 + 3H]^{5+}$) agree to within <7 ppm with the theoretical mass-to-charge ratios for these species (1470.59, 1473.59, 1476.59, and 1479.59 respectively). Fe-bound trimers are also observed in the 4+ charge state. The measured mass-to-charge ratios were 1837.98 and 1849.24 for $[^{56}Fe(\alpha pL_{V1})_3 + 3H]^{4+}$ and $[^{56}Fe(\alpha pL)_3 + 3H]^{4+}$, respectively. Those values agree to within <6 ppm of the theoretical values (*m*/*z* 1837.99 and 1849.24). Thus, the formal 2+ oxidation state of the Fe is retained in the gas phase and the remaining charge arises from the attachment of two (4+ charge state) or three (5+ charge state) protons. Evidence for the retention of the 2+ oxidation state in tris(2,2′-bipyridyl)iron(II) coordination complexes following electrospray has previously been shown by Posey and co-workers.[65] Doubly and triply charged monomeric species are also observed in Figure 1 (middle), as are the 3+ and 4+ dimers without bound iron (*m*/*z* ~1630 and 1240). The stoichiometries chosen for this experiment suggest that 40% of the total peptides should remain monomeric, as qualitatively observed experimentally.

Stability Screening of Metal-Ion Selected Dynamic Protein Libraries. (I) αpL/αpL_{V1} Library. The simplest dynamic library arises through the assembly of two differing peptide subunits. Chelation of Fe(II) by peptides αpL and αpL_{V1} results in four possible species: $Fe(\alpha pL)_3$, $Fe(\alpha pL_{V1})_3$, $Fe(\alpha pL)_2(\alpha pL_{V1})$, and $Fe(\alpha pL)(\alpha pL_{V1})_2$. The folding free energies, ΔG_{fold}, for exchange-inert ruthenium(II) analogues, $Ru(\alpha pL)_3$ and $Ru(\alpha pL_{V1})_3$, are -3050 ± 100 and -2000 ± 100 cal/mol, respectively, suggesting that trihelix bundles of peptide αpL are more stable than those of peptide αpL_{V1}. These free energies suggest that all four species should be present in an equilibrium mixture of Fe(II) trihelix bundles.

The first step in analyzing the relative stabilities of various Fe-bound trihelix bundles by screening of dynamic libraries with ESI FT-ICR MS is to examine the relative abundances of various Fe-bound trimers as a function of Fe(II) concentration. In the first instance, the mass spectrum provides a "snapshot" of the stable trihelix bundles. (Note that the gas-phase species do not necessarily have the same structures as the solution-phase species). At low Fe(II) concentration, the most stable trihelix bundle will be favored. Increasing the Fe(II) concentration allows less stable bundles to form. An inherent assumption is that the ESI efficiency does not vary between these species. Although ESI efficiency can differ markedly[66] for molecules of different basicity (positive-ion ESI) or acidity (negative-ion ESI), in the present case the charge on the trimers arises from the Fe^{2+} and attachment of two (4+ charge state) or three (5+ charge state) protons to peptide subunits. The peptide subunits have identical basic amino acid residues, and therefore, ESI basicity suppression effects should not affect the relative abundances of stable complexes.

Figure 2 shows mass spectral segments (chosen to show the 5+ charge state of the Fe-bound trimers) for the αpL/αpL_{V1} library at each of four Fe(II) concentrations. The same distributions of trimers with respect to Fe(II) concentration were observed for the +4 charge state (not shown). Note that each spectrum is vertically scaled relative to its highest-magnitude peak. Thus, although the absolute concentration of $Fe(\alpha pL)_3$ increases asymptotically as Fe(II) concentration increases, the

(65) Burns, T. D.; Spence, T. G.; Mooney, M. A.; Posey, L. A. ESI of divalent transition metal ion bipyridine complexes: evidence for preparation of solution analogs in the gas phase. *Chem. Phys. Lett.* **1996**, *258*, 669−679.

(66) Mann, M. Electrospray—its potential and limitations as an ionization method for biomolecules. *Org. Mass Spectrom.* **1990**, *25*, 575−587.

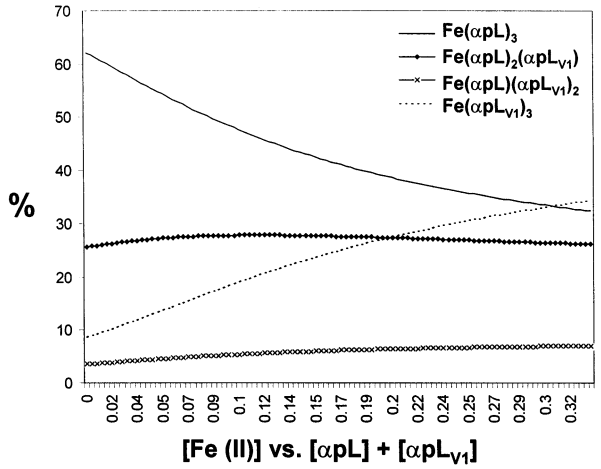

Figure 3. Modeled plot of relative abundance of trimers $Fe(\alpha pL)_3$, $Fe(\alpha pL)_2(\alpha pL_{V1})$, $Fe(\alpha pL)(\alpha pL_{V1})_2$, and $Fe(\alpha pL_{V1})_3$ versus ratio of Fe(II) concentration to total peptide concentration, i.e., $[\alpha pL] + [\alpha pL_{V1}]$, determined from trihelix folding free energies: ΔG_{fold}, −3.05(0.1) kcal mol^{-1} ($(\alpha pL)_3$); −2.00(0.1) kcal mol^{-1} ($(\alpha pL_{V1})_3$); −2.2(0.1) kcal mol^{-1} ($(\alpha pL)_2(\alpha pL_{V1})$); −1.1(0.1) kcal mol^{-1} ($(\alpha pL)(\alpha pL_{V1})_2$).

$Fe(\alpha pL)_3$ concentration decreases relative to other species. At the lowest iron concentration ($^1/_{30}$ equiv of Fe(II), Figure 1, top), the dominant Fe-bound species is the homotrimer $Fe(\alpha pL)_3$. As the Fe(II) concentration increases, the relative abundance of the heterotrimer $Fe(\alpha pL)_2(\alpha pL_{V1})$ increases. The heterotrimer $Fe(\alpha pL)(\alpha pL_{V1})_2$ is also observed. At $^1/_5$ and $^1/_3$ equiv of Fe(II), the dominant species are the homotrimers $Fe(\alpha pL_{V1})_3$ and $Fe(\alpha pL)_3$. At $^1/_3$ equiv of Fe(II), all peptides can be incorporated within trihelix bundles. The relative abundance of free peptide (combined 2+ and 3+ charge states) in the mass spectrum is ~2%. Thus, significant dissociation of the trimers does not occur during the electrospray process, and given that little or no peptide exchange occurs after the ionization of the sample, the mass spectra are expected to sample the solution-phase distribution of species. The variation in trimer distributions with Fe(II) concentration can be modeled by assuming a total free energy of complex formation as the sum of two processes. The first process is the association of Fe(II) with the three bipyridyl ligands. This term is the same for all the complexes and may be assumed to be about −20 kcal mol^{-1}.[63,64] The second process is the free energy of folding of the trihelix and depends on the quality of the folded structure. For this library, the solution folding free energies of the exchange-inert homotrimers $Ru(\alpha pL)_3$ and $Ru(\alpha pL_{V1})_3$ were experimentally determined, through circular dichroism experiments, to be −3.05 (0.1) and −2.00 (0.1) kcal mol^{-1}, respectively, as described above. (Analysis of exchange-inert homotrimers allows deconvolution of the contribution of free energy of folding of the trihelix.) With those numbers in hand, it is interesting to ask whether the unknown folding free energies of the heterotrimers may be predicted from the distribution of species observed in the mass spectra. Fitting a calculated distribution of species to the observed distribution returned by the mass spectra suggests respective folding free energies of −2.2 (0.1) and −1.1 (0.1) kcal mol^{-1} for the heterotrimers $Fe(\alpha pL)_2(\alpha pL_{V1})$ and $Fe(\alpha pL)(\alpha pL_{V1})_2$. Figure 3 shows the modeled distribution of species with Fe(II) concentration determined from these folding free energies. The distribution agrees well with that observed (Figure 2).

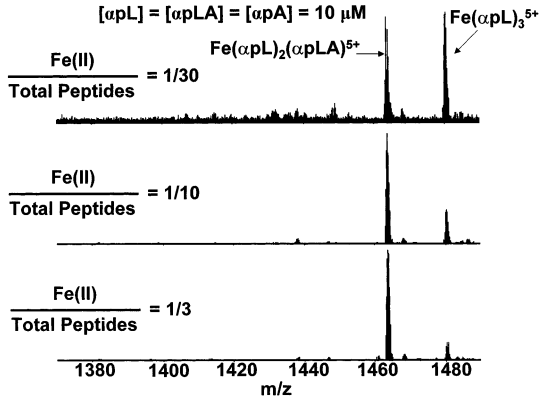

Figure 4. Mass spectral segments showing 5+ charge state of Fe-bound trimers obtained from samples containing peptides αpL (10 μM), αpLA (10 μM), and αpA (10 μM) and (top) 1 μM Fe(II), (middle) 3 μM Fe(II), and (bottom) 10 μM Fe(II).

The variation of Fe-bound trimer distributions at different Fe(II) concentrations observed in the ESI FT-ICR mass spectra suggests that the complexes containing αpL form more stable trihelix bundles than those complexes containing αpL_{V1}, with an optimal packing stability order of $Fe(\alpha pL)_3 > Fe(\alpha pL)_2(\alpha pL_{V1}) > Fe(\alpha pL_{V1})_3 > Fe(\alpha pL)(\alpha pL_{V1})_2$. The higher stability of the αpL complexes relative to the αpL_{V1} complexes is not especially predictable. Both αpL (Bpy-GELAQKLEQALQK-LEQALQK-NH_2) and αpL_{V1} (Bpy-GQAVQKLEQALQKLE-QALQK-NH_2) are leucine-rich at the hydrophobic a- and d-positions.[26,67,68]. The first a-position is occupied by an alanine in αpL and by a valine in αpL_{V1}. It is worth noting that the residues adjacent to the first a-position, i.e., those at the g-position, are leucine and alanine for αpL and αpL_{V1}, respectively. Even though the g-position leucine of αpL is out of register, it could still contribute to the hydrophobic core, leading to a more stable complex.

(II) αpL/αpLA/apA library. In our second study, we consider the library arising through the assembly of three peptide subunits, αpL, αpLA, and αpA, with the sequence, Bpy-GEL-$AQKX_1EQAX_2QKX_3EQAX_4QK$-$NH_2$ in which X represents a variable amino acid residue at hydrophobic core a- and d-positions.[26,67,68] For αpL, X = leucine. For αpLA, X_1, X_3 = alanine; X_2, X_4 = leucine. For αpA, X = alanine. In this library, all peptides possess glutamic acid at position 2, and any differences in trimer stability arise as a result of subunit packing. Given the hydrophobicity of the leucine residue, the leucine-rich peptides would be expected to yield the most stable trimeric complexes. Previous work by Case and McLendon[20] showed that of the 11 candidate trimers in this library,[69] only two form trihelix bundles: $Fe(\alpha pL)_3$ and $Fe(\alpha pL)_2(\alpha pLA)$.

Figure 4 shows mass spectral segments (chosen to show the 5+ charge state of the Fe-bound trimers) obtained from the αpL/αpLA/apA library at each of three ferrous iron concentrations. The relative distribution of trimers in 5+ charge state as a function of Fe(II) concentration was the same, to within

(67) Gonzalez, L. J.; Woolfson, D. N.; Alber, T. Buried polar residues and structural specificity in the GCN4 leucine zipper. *Nat. Struct. Biol.* **1996**, *3*, 1011−1018.
(68) Gonzalez, L. J.; Brown, R. A.; Richardson, D.; Alber, T. Crystal structures of a single coiled-coil peptide in two oligomeric states reveal the basis for structural polymorphism. *Nat. Struct. Biol.* **1996**, *3*, 1002−1009.
(69) There are actually 44 members of the virtual library when one considers the facial, meridional, Δ, and Λ stereochemistries possible at the metal center. We have considered only the Λ facial topoisomers.

experimental error, as that observed for the 4+ charge state (not shown). At $^1/_{30}$ total peptide equivalent (i.e., 1 μM Fe(II); see Figure 2 (top)), the only Fe-bound trimers are the homotrimer Fe(αpL)$_3$ and the heterotrimer Fe(αpL)$_2$(αpLA). The measured *m*/*z* values, 1479.59 for [^{56}Fe(αpL)$_3$ + 3H]$^{5+}$ and 1462.76 for [^{56}Fe(αpL)$_2$(αpLA) + 3H]$^{5+}$, are in good agreement with the calculated values (1479.59 and 1462.77, respectively). This result suggests that of the 11 members of this virtual trihelix library, the leucine-rich bundles are the most stable. As the concentration of Fe(II) increases relative to those of the peptides involved in the stable complexes, the equilibrium shifts toward the heterotrimer Fe(αpL)$_2$(αpLA). This observation is a consequence of approaching the limiting concentration of peptide αpL, in accordance with Le Chatelier's principle. Thus, at $^1/_{10}$ equiv of Fe(II) (Figure 4 (middle)), the stable Fe(αpL)$_2$(αpLA) and Fe(αpL)$_3$ trimers are observed, but with higher abundance of the heterotrimer relative to the homotrimer. Figure 4 (bottom) shows the results obtained when a stoichiometric amount of Fe(II), i.e., $^1/_3$ equiv, was added to the peptide mixture. It is notable that even at the highest Fe(II) concentration, the dominant species are still Fe(αpL)$_2$(αpLA) and Fe(αpL)$_3$ although all peptides could in principle be sequestered; i.e., trisbipyridyl complexes that are not observed to fold could be present. The remaining Fe-bound trimers, which are known from circular dichroism studies not to exist as trihelices, are detected only in very low abundance in this spectrum. The observation that only species that correspond to stable trihelix bundles are observed in the mass spectra is a particular advantage. The automatic elimination of nontrihelical candidates in a larger library would be very useful because it would allow rapid screening. This observation also means that despite the results for the αpL/αpL$_{V1}$ library, the absolute solution-phase equilibrium distributions cannot be determined from the ESI FT-ICR mass spectra in all cases.

As noted above, the present library has previously been screened by size-exclusion chromatography followed by mass spectrometric analysis to identify subunit peptides.[20] Exchange-inert ruthenium(II) analogues of the complexes were synthesized, and their folding free energies were determined.[20] The mass spectrometric results shown in this paper agree with those of previous studies, confirming our expectation that the leucine-rich peptides combine to form bundles of higher stability.

Infrared Multiphoton Dissociation of Homotrimeric Trihelix Bundles. Once an optimally stable bundle has been selected from a large library, identification of each peptide will in general require its dissociation to yield fragments from which amino acid sequences can be reconstructed. Infrared multiphoton dissociation (IRMPD) of the homotrimers Fe(αpL$_{V1}$)$_3^{5+}$ and Fe(αpL)$_3^{5+}$ (Figure 5) yields primarily the doubly protonated peptide monomer and the triply charged (singly protonated) Fe-bound dimer. The calculated *m*/*z* for (^{56}Fe(αpL$_{V1}$)$_2$ + H)$^{3+}$ is 1639.87, and the measured *m*/*z* is 1639.88. The calculated *m*/*z* for (^{56}Fe(αpL)$_2$ + H)$^{3+}$ is 1649.87 and the measured *m*/*z* is 1649.87.

Partial sequence information about the peptide subunit may be revealed by MS^3 on either monomer or Fe-bound dimer. Figure 6 (top) shows the FT-ICR MS^3 mass spectrum following IRMPD of the doubly charged αpVL^{2+} monomer isolated following IRMPD of the homotrimer, Fe(αpVL)$_3^{5+}$. Some of the more abundant backbone fragments are labeled. The

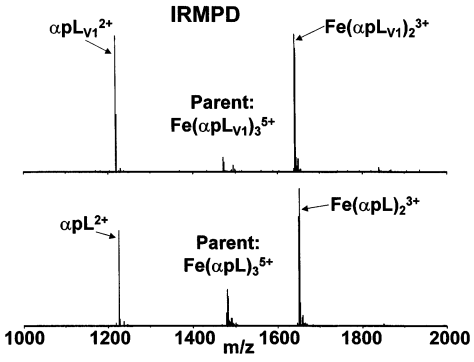

Figure 5. ESI FT-ICR mass spectra following infrared multiphoton dissociation (IRMPD) of Fe-bound homotrimers: (top) Fe(αpL$_{V1}$)$_3^{5+}$; (bottom) Fe(αpL)$_3^{5+}$.

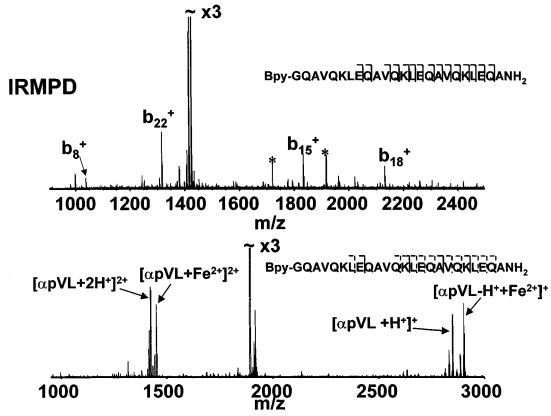

Figure 6. ESI FT-ICR mass spectrum following IRMPD of (top) αpVL^{2+} monomer (generated by prior IRMPD of the homotrimer, Fe(αpVL)$_3^{5+}$) and (bottom) Fe(αpVL)$_2^{3+}$ (generated by prior IRMPD of the homotrimer Fe(αpVL)$_3^{5+}$). Each inset shows the observed b-cleavages. The asterisk (∗) respresents species not removed by SWIFT isolation. Dashed lines indicate cleavages observed in both free and Fe-bound monomer.

numerous backbone b-cleavages corresponding to b$_8^+$, b$_9^+$, b$_{11}^+$−b$_{19}^+$, and b$_{18}^{2+}$−b$_{23}^{2+}$ (see inset) provide extensive sequence information. The lack of y-ions may be attributed to the basicity of the bipyridyl group: i.e., positive charge is retained on the N-terminus. Figure 6 (bottom) shows the FT-ICR MS^3 mass spectrum following IRMPD of the triply charged (singly protonated) Fe-bound dimer Fe(αpVL)$_2^{3+}$ isolated following IRMPD of the homotrimer Fe(αpVL)$_3^{5+}$. The most abundant fragments are singly and doubly protonated monomer ions. Fe-bound monomer ions, [αpVL + Fe]$^{2+}$ and [αpVL − H + Fe]$^+$, are also observed. Again, numerous backbone b-cleavages may be identified, b$_7^+$, b$_8^+$, b$_{12}^+$−b$_{20}^+$, b$_{22}^+$, b$_{19}^{2+}$, and b$_{21}^{2+}$−b$_{23}^{2+}$, as well as peaks corresponding to the Fe-bound b-ions, (b$_7$ − H + Fe)$^+$, (b$_{12}$ − H + Fe)$^+$, (b$_{14-16}$ − H + Fe)$^+$, (b$_{18-19}$ − H + Fe)$^+$, (b$_{22-23}$ − H + Fe)$^+$, and (b$_{21-23}$ + Fe)$^{2+}$. Cleavages (see inset) labeled by a dashed line are observed for both free and Fe-bound peptides.

Infrared Multiphoton Dissociation of Heterotrimeric Trihelix Bundles. IRMPD of the heterotrimers was also performed. The principal products from IRMPD of the heterotrimer Fe(αpL)$_2$(αpL$_{V1}$)$^{5+}$ (Figure 7, top) are singly protonated Fe(αpL)$_2^{3+}$ and Fe(αpL)(αpL$_{V1}$)$^{3+}$ and doubly protonated αpL^{2+} and αpL$_{V1}^{2+}$, as expected from previous experiments. The theoretical mass-to-charge ratios for (^{56}Fe(αpL)(αpL$_{V1}$) + H)$^{3+}$ and (^{56}Fe(αpL)$_2$ + H)$^{3+}$ are 1644.87 and 1649.87, and the measured values are 1644.87 and 1649.87. Statistically, one

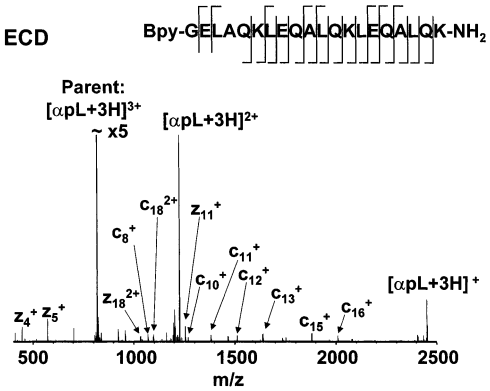

Figure 7. ESI FT-ICR mass spectra following IRMPD of the Fe-bound heterotrimers (top) $Fe(\alpha pL)_2(\alpha pL_{V1})^{5+}$ and (bottom) $Fe(\alpha pL)(\alpha pL_{V1})_2{}^{5+}$.

might expect that the relative abundance of the heterodimer $Fe(\alpha pL)(\alpha pL_{V1})^{3+}$ would be twice that of the homodimer $Fe(\alpha pL)_2{}^{3+}$ and that the relative abundance of monomer αpL^{2+} would be twice that of $\alpha pL_{V1}{}^{2+}$. Therefore, the observation that the homodimer and heterodimer have approximately the same abundance suggests that the homodimer is more stable than the heterodimer and that the species exhibit some secondary structure in the gas phase. IRMPD of the $Fe(\alpha pL)(\alpha pL_{V1})_2{}^{5+}$ heterotrimer (Figure 6, bottom) yields $Fe(\alpha pL)(\alpha pL_{V1})^{3+}$ and $\alpha pL_{V1}{}^{2+}$ ($^{56}Fe(\alpha pL)(\alpha pL_{V1}) + H)^{3+}$ theoretical *m*/*z* is 1644.87; measured *m*/*z* is 1644.88). The signal/noise of the peak corresponding to $(^{56}Fe(\alpha pL_{V1})_2 + H)^{3+}$ was too low for accurate mass measurement. Clearly, the heterodimer $Fe(\alpha pL)(\alpha pL_{V1})^{3+}$ is much more abundant than the homodimer $Fe(\alpha pL_{V1})_2{}^{3+}$, suggesting that $Fe(\alpha pL)(\alpha pL_{V1})$ is a more stable dimer than $Fe(\alpha pL_{V1})_2$ and again providing evidence for secondary structure in the gas phase. It is important to reiterate that the relative dimer stabilities discussed here are inferred from gas-phase measurements. Recent work by McLafferty and co-workers[70] showed that ubiquitin refolds to a predominantly helical structure in the gas phase. It would not be surprising if the complexes in our study behaved similarly, given that they are designed to be exclusively α-helical. The gas-phase experiments effectively sample the solution-phase equilibrium distribution of stable species.[37] Any retention of a specific solution-phase coiled-coil structure in the gas phase is likely to be a consequence of our choice of helical secondary structure. Finally, it is also conceivable that the higher stability of gas-phase dimers incorporating αpL arises through interactions of the glutamate side chain (position 2) with the metal center.

Electron Capture Dissociation. Figure 8 shows the FT-ICR mass spectrum following electron capture dissociation (ECD)[44,45] of the αpL^{3+} monomer. The most abundant species are the charge-reduced ions $[\alpha pL + 3H]^{2+}$ and $[\alpha pL + 3H]^{+}$ (i.e., capture of one or two electrons without dissociation). In addition, the numerous c and z backbone cleavages (see inset: $z_4{}^{+}-z_6{}^{+}$, $z_{10}{}^{+}$, $z_{11}{}^{+}$, $z_{14}{}^{+}$, $z_{18}{}^{2+}$, $z_{19}{}^{2+}$, $c_5{}^{+}-c_{19}{}^{+}$, and $c_{17}{}^{2+}-c_{19}{}^{2+}$) yield extensive sequence information.

ECD of the triply protonated iron complex, $Fe(\alpha pL)_3{}^{5+}$ (Figure 9), yields primarily the charge-reduced species $[Fe(\alpha pL)_3 + 3H]^{4+}$, $[Fe(\alpha pL)_3 + 3H]^{3+}$, and $[Fe(\alpha pL)_3 + 3H]^{2+}$, along with species corresponding to amino acid side chain losses,[71] notably the loss of 45 Da from glutamine. Limited sequence information (see inset) is available from the observed c fragments, $c_{15}-c_{19}$, in the C-terminal region. (It is worth noting that those c-cleavages occur within peptide subunits still bound in the trimer complex.) These observations provide further evidence for secondary structure in the gas phase; i.e., noncovalent interactions are evidently holding the complex together, preventing observation of fragments due to c/z cleavage along the peptide backbone. As discussed earlier, the most plausible explanation for this observation is partial retention of solution-phase structure, but it is possible that the secondary structure is derived from noncovalent interactions between rearranged peptide subunits. Only at the C-terminus of the complex are backbone fragments observed. Note that the charge on the monomer ion subjected to ECD (Figure 8) is 3+, provided by the attachment of three protons. If it is assumed that one proton resides on the bipyridyl moiety, given its basicity, the remaining two protons will reside on basic amino acids in the peptide. The charge on the trihelix complex was 5+. The iron contributes 2+, so the remaining charge arises from three protons distributed over *three* peptide subunits. Thus, the more extensive cleavage observed for ECD of the monomer could in part be attributed to its higher positive charge. However, that would not explain the confinement of c-cleavage to the C-terminal region of the complex. The extensive side chain cleavage also suggests that electron capture is occurring throughout the peptide. We

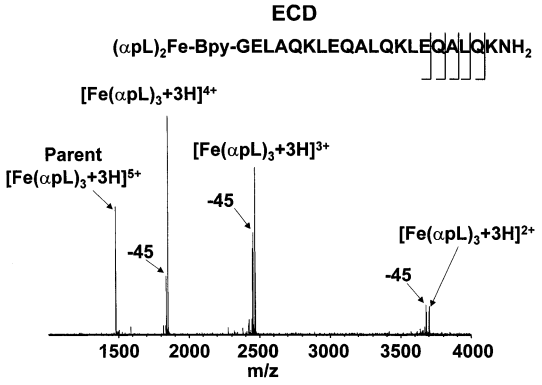

Figure 8. ESI FT-ICR mass spectrum following ECD of the αpL^{3+} peptide monomer. Major fragments are indicated. Inset: c and z cleavages.

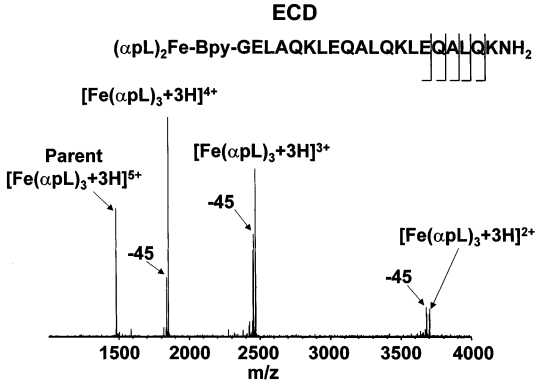

Figure 9. ESI FT-ICR mass spectrum following ECD of the triply protonated complex $Fe(\alpha pL)_3{}^{5+}$. Inset: c and z cleavages.

(70) Oh, H.; Breuker, K.; Sze, S.-K.; Ge, Y.; Carpenter, B. K.; McLafferty, F. W. Secondary and tertiary structures of gaseous protein ions characterized by ECD mass spectrometry and photofragment spectroscopy. *Proc. Natl. Acad. Sci. U.S.A.* **2002**, *99*, 15863−15868.

(71) Cooper, H. J.; Hudgins, R. R.; Hakansson, K.; Marshall, A. G. Characterization of amino acid side chain losses in electron capture dissociation. *J. Am. Soc. Mass Spectrom.* **2002**, *13*, 241−249.

therefore attribute the lack of backbone cleavages in the complex to the existence of secondary structure in the gas phase, possibly due to partial retention of the solution-phase coiled-coil structure. Unfortunately, such strong noncovalent interactions may limit the sequence information available from ECD of the trihelix complexes. It may become necessary to combine the two dissociation techniques for application to larger libraries, i.e., to employ IRMPD to generate the peptide monomers and then perform ECD to gain sequence information. Such a strategy would, in principle, enable unambiguous amino acid sequence determination of any trihelix bundle in toto.

Conclusion

The present results demonstrate the suitability of ESI FT-ICR mass spectrometry as a technique for investigating the relative stabilities and packing efficiencies of trihelix bundles in a metal-ion selected dynamic protein library. Synthesis of exchange-inert analogues and measurement of their folding free energies confirm the identities of optimally stable candidate trimers returned by ESI FT-ICR. From a library of candidate trimers, only those corresponding to trihelix bundles are returned in the mass spectra, as demonstrated in the αpL/αpLA/αpA library. Relative stabilities of trihelix bundles can be determined from their distributions at various Fe(II) concentrations, as evidenced in the αpL/αpL$_{V1}$ library. It is also worth noting that these results constitute the first direct mass spectrometric observation of exchange-labile trihelix bundles. Electron capture dissociation of peptide monomers provides extensive sequence information. Sequence information could also be obtained from IRMPD MS^3 experiments. However, ECD of the Fe-bound complexes yielded little sequence information presumably because of the existence of secondary structure in the gas phase. Evidence for gas-phase secondary structure comes from the IRMPD of the Fe-bound heterotrimers. IRMPD of Fe-bound heterotrimers also provides previously unavailable information about the Fe-bound dimers in these systems. Microelectrospray FT-ICR MS, supported by IRMPD and ECD, not only resolves and establishes the relative stabilities of trihelix bundles but also identifies their constituent peptides. We project that these techniques will form a strong basis for characterizing larger dynamic libraries and further addressing the question of optimal packing in noncovalent macromolecular assemblies.

Acknowledgment. This work was supported by the NSF National High-Field FT-ICR Mass Spectrometry Facility (Grant CHE 99-09502), Florida State University, the National High Magnetic Field Laboratory at Tallahassee, Florida (H.J.C. and A.G.M.), and the National Science Foundation (Grant CHE 01-06342) (M.A.C. and G.L.M.).

JA021138F